Proceedings of the ASME 2011 Pressure Vessels & Piping Division Conference
PVP2011
July 17-21, 2011, Baltimore, Maryland, USA

PVP2011-57645

NRC/EPRI Welding Residual Stress Validation Program - Phase III Details and Findings

Lee F. Fredette*

Battelle Memorial Institute, Columbus, Ohio

John E. Broussard

Dominion Engineering Inc., Reston, VA

Matthew Kerr, Howard J. Rathbun‡

US Nuclear Regulatory Commission
Office of Nuclear Regulatory Research, Washington, DC

ABSTRACT

The US Nuclear Regulatory Commission (NRC) and the Electric Power Research Institute (EPRI) are working cooperatively under a memorandum of understanding to validate welding residual stress predictions in pressurized water reactor primary cooling loop components containing dissimilar metal (DM) welds. These stresses are of interest as DM welds in pressurized water reactors are susceptible to primary water stress corrosion cracking (PWSCC) and tensile weld residual stresses are one of the primary drivers of this stress corrosion cracking mechanism. The NRC/EPRI welding residual stress (WRS) program currently consists of four phases, with each phase increasing in complexity from lab size specimens to component mock-ups and ex-plant material.

This paper discusses Phase III of the WRS characterization program, comparing measured and predicted weld residual stresses profiles through the dissimilar metal weld region of pressurizer safety and relief nozzles removed from a cancelled plant in the United States. The DM weld had already been completed on all of the plant nozzles before use in the mock-up program. One of the nozzles was completed with the application of the stainless steel safe-end weld to a section of stainless steel pipe. Measurements were taken on the nozzles with and without the welded pipe section. Several independent finite element analysis predictions were made of the stress state in the DM weld. This paper compares the predicted stresses to those found by through-thickness measurement techniques (Deep Hole Drilling and Contour Method). Comparisons of analysis results with experimental data will allow the NRC staff to develop unbiased measures of uncertainties in weld residual stress predictions with the goal of developing assurances that the analysis predictions are defensible through the blind validation provided using well controlled mock-ups and ex-plant material in this program.

INTRODUCTION

In pressurized water reactor (PWR) coolant systems, nickel based dissimilar metal (DM) welds are typically used to join carbon steel components, including the reactor pressure vessel (RPV), steam generators (SGs), and the pressurizer to stainless steel piping. Figures 1 and 2 show a representative nozzle to piping connection and cross section including the DM weld indicated as Alloy 82 in the figures. The DM weld is fabricated by sequentially depositing weld beads as high temperature molten metal that cools, solidifies, and contracts retaining stresses that approach, or potentially, exceed the material's yield strength. These DM welds are susceptible to primary water stress corrosion cracking (PWSCC) as an active degradation mechanism that has led to reactor coolant system pressure boundary leakage. Weld residual stresses (WRS) are the dominant mechanical driving force for crack initiation and propagation within the DM weld material due to PWSCC. Hence, proper assessment of these stresses is essential to accurately predict PWSCC flaw growth and ensuring component integrity. Sources of variability in WRS include fabrication, repair and PWSCC mitigation processes.

* Responsible Author: Battelle 505 King Ave., Columbus, Ohio 43201 E-mail: Fredette@battelle.org Phone: 614-424-4462 Fax: 614-424-3228

‡ The views expressed herein are those of the authors and do not represent an official position of the U.S. NRC or Battelle Memorial Institute.

A cooperative research program was developed between the NRC and industry to address this complicated issue. The NRC and the Electric Power Research Institute (EPRI) signed a memorandum of understanding which allowed and encouraged cooperation in nuclear safety research that provides benefit for both the NRC and industry. The memorandum of understanding is authorized pursuant to Section 31 of the Atomic Energy Act and/ or Section 205 of the Energy Reorganization Act [1].

The objectives of the NRC/EPRI sponsored research can be described as six fold. The program will help the US NRC Office of Nuclear Regulatory Research (RES) in developing appropriate WRS flaw evaluation review guidelines. It will allow the performance of independent confirmatory research on industry guidance for performing WRS analyses. It will assess and evaluate near-term adequacy of industry's mitigation activities where WRS minimization is necessary. The research is intended to improve WRS finite element analysis predictive methodologies. The final two related goals are the subject of this paper: To assess variability of WRS predictions and measurements and to determine estimates of the uncertainty and distribution of WRS which are needed as inputs in the probabilistic analysis code that the NRC and EPRI are currently developing (xLPR– eXtremely Low Probability of Rupture)[2]

The approach of the research program is to use blind validation of both finite element predictions and measurement techniques using a series of well controlled mock-ups and actual plant components. The program was divided into four phases with mock-ups of increasing complexity and similarity to actual plant components. Phase I consisted of welded flat plate and simple welded cylinders. Phase II consisted of two fabricated prototypic surge nozzle geometries. Phase III consisted of actual pressurizer safety and relief nozzles and will be the subject of this paper. The Phase IV mock-up used a cold leg nozzle from a canceled plant and was used to validate the effect of safe end welding and optimized weld overlay as a WRS mitigation method.

The Phase III mock-ups will be discussed in this paper. Results from six different finite element models will be compared to through-thickness weld residual stress measurements in the DM weld area. The through-thickness stress measurements were performed by the deep hole drilling method by Veqter, LTD. [3,4] and by the contour method by Hill Engineering, LLC. [5]. The finite element analyses and the measurements were done independently. Also, the finite element models were created with a minimum of information provided. Mock-up measurements, materials, and a micrograph were provided as background information to the modelers.

PHASE III MOCK-UP

The Phase III mock-up components discussed here consisted of two safety and relief nozzles from the pressurizer of a canceled plant. Residual stress measurements were taken before and after the application of the stainless steel pipe weld. Two different nozzles were needed to accomplish this because of the destructive nature of the contour method stress measurement technique. Figure 1 shows a schematic of the nozzle after the stainless steel weld was put in place to join the nozzle to a piece of stainless steel pipe. The DM weld is indicated at the location of the Alloy 82 Butter and Weld material.

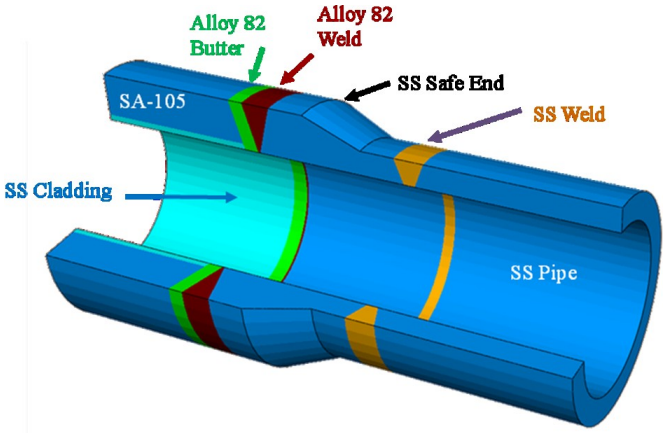

Figure 1. Schematic of the Safety and Relief Nozzle

Figure 2 shows one of the actual nozzles and one of the finite element representations of it in the state both before and after the stainless steel pipe weld to the safe end. The nozzle without the stainless steel pipe will be called Nozzle #2, and the nozzle with the stainless steel pipe weld will be called Nozzle #3 throughout this paper.

The two nozzles used for measurements were slightly different leading to variation in the measurements between the two nozzles. Each nozzle had its DM weld completed and was prepared for the subsequent stainless steel weld to pipe section before it was removed from the canceled plant.

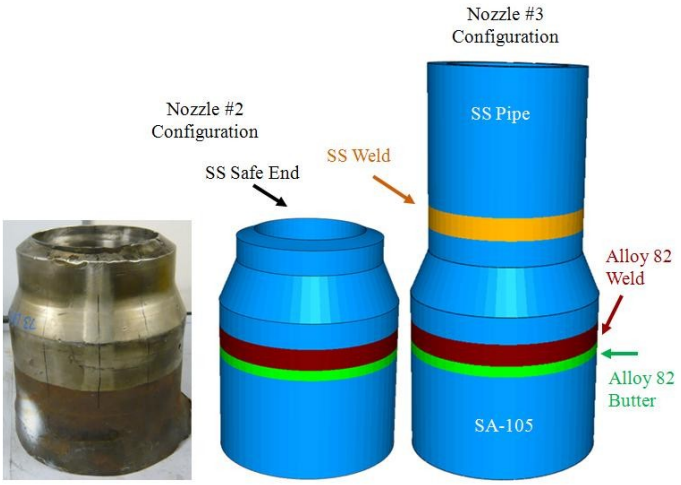

Figure 2. Actual Nozzle and FEA Model Before and after Pipe Weld

As described in [5] Nozzle #2 was 375 mm long with a 203 mm outer diameter and a 133 mm inner diameter. Nozzle #3 was 711 mm long with a 201 mm outer diameter and an inner diameter of 113 mm.

FEA MODELS

Four different analysts created finite element models using measurements reported and by scaling dimensions from micrographs taken at the planes where the contour method cuts were made. Each model is slightly different due to the differences in the nozzles themselves and the differences in the scaled dimensions used. Results are reported as through-thickness stresses with the distance through the thickness normalized to take out the variation in wall thickness in the models and the actual nozzles.

Other variations in the models are typical of those that would occur in industry when various modelers make FEA predictions of the same geometry. The meshes were different. The butter and DM weld beads were visible in the micrographs provided and each modeler made assumptions as to the welding bead shape to use in their FEA model. Two different software packages were used (ANSYS and ABAQUS). The nozzle component materials were known, but modelers used their own library of material properties representing behavior over the range of the welding process temperatures. Also, different hardening laws were used for the materials making a total of nine through-thickness stress predictions using either isotropic material hardening, linear isotropic hardening, kinematic hardening, mixed hardening or elastic-perfectly plastic material behavior. In all cases, thermal models were calibrated against the provided weld micrographs, but the number and specific geometry of the weld passes modeled varied from analyst to analyst.

Figures 3 and 4 show the results of the nine finite element predictions for axial and hoop stress through the thickness of the centerline of the DM weld. These results will later be compared to the measurements at the same location. The results are for the case after the stainless steel pipe weld was performed (Nozzle #3 configuration). Each of the modelers found that, for this geometry, there was almost no difference in the DM weld through-thickness stress before and after the stainless steel weld was performed. Stresses were different elsewhere in the models but the DM weld through-thickness stresses were essentially unchanged by the application of the stainless steel weld. This fact is attributed to the reduction in diameter and thus wall thickness at the stainless steel pipe, and the distance of the stainless steel weld from the DM weld (126 mm [4]). The safe-end stainless steel weld usually provides some reduction in the DM weld stresses in more uniform geometries as shown in previous studies [6,7,8,9].

First, a description of the graphs is in order since this format will be used for the subsequent comparisons as well. Each modeler, and each measurement technique, for that matter, reported a different number of data points through the thickness of the nozzle. These differences were because of the differences in models, meshes, and measurement techniques. The data provided from all models and measurements was linearly interpolated between provided data points to create 50 even steps through the thickness so that tabulated results could be compared directly. Averages and standard deviations were created at each step through the thickness. The graphs show the running average of the data presented as a thick blue line through the center of the data plots. The actual data is shown as thin color-coded lines in these graphs, and the data is enveloped in two red dashed lines which represent the ± 3-standard deviation bound on the data provided. Therefore 99.7% of the data points should fall within the ± 3-standard deviation bounds.

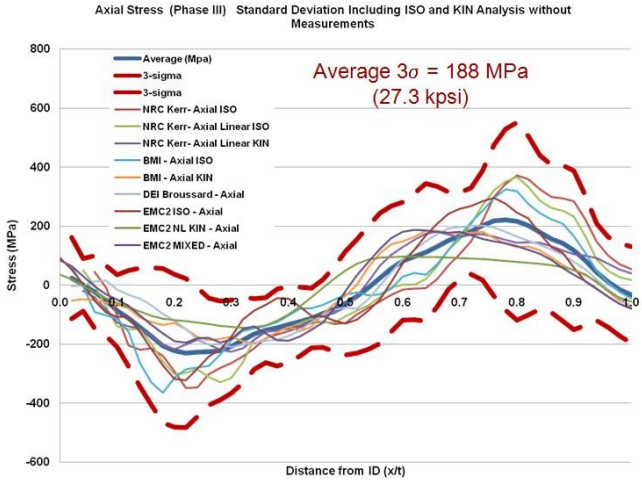

Figure 3. Axial Stress FEA Predictions through the Centerline of the DM Weld

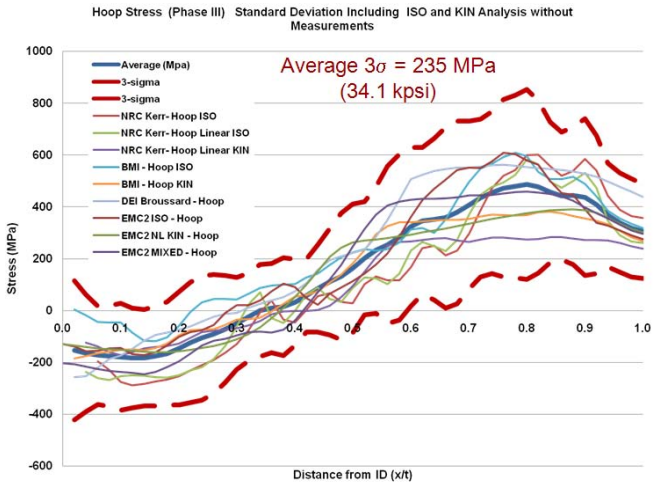

Figure 4. Hoop Stress FEA Predictions through the Centerline of the DM Weld

Several observations can be made from these prediction comparisons. All of the results show similar trends. The

average curve shows the inner diameter axial stress is near neutral and then dips into the compressive region until it becomes tensile at 50% through the thickness and finally becomes neutral again at the outer diameter. The hoop stress average curve shows the stresses to be compressive at the inner diameter and tensile at the outer diameter with the curves crossing into tension somewhat before 50% through the thickness from the inner diameter.

The curves of stresses provided from the models using isotropic hardening can be clearly distinguished from those using kinematic hardening. The hardening law used for each prediction is indicated in the legend text as ISO, KIN, Mixed, or in the case of the DEI results, elastic-perfectly plastic material behavior. The annealed mid-range yield strength for the Alloy 82 DM weld is 265 MPa (38.4 ksi). The differences come about because of the strain cycles created in the welding process. The models following the isotropic hardening law allow the material to strain harden to progressively higher yield strength upon cyclic loading and this produces higher stresses than does the kinematic hardening law. One can observe that the results produced with kinematic hardening do not exceed the stress equivalent to the annealed yield strength of the material by nearly as much as the results from the models using the isotropic hardening law. This difference is expected and is indicated in the bulges in the ± 3-standard deviation enveloping curves for both the axial and hoop stress predictions. The effect is most noticeable in the axial stress graph where the isotropic models produce high compression stresses at 20% through the thickness, and high tension stresses at 80% through the thickness while the kinematic models produced more damped stress swings.

Though the prediction trends are very similar, the ±3-standard deviation curves show that there can be significant differences produced from small variations in modeling practice. The average ±3-standard deviation range for the axial stresses through the thickness is ±188 MPa (27.3 ksi), and the average for the hoop stresses through the thickness is ±243 MPa (35.2 ksi).

MEASUREMENTS

Several types of residual stress measurement techniques were used on the mock-up nozzles, but only the methods which produced through-thickness measurements will be discussed here and compared with the FEA predictions. Two techniques were used by two independent providers. The Deep Hole Drilling method (DHD), and its variant, the incremental Deep Hole Drilling method (iDHD) were performed on the nozzle mock-ups by Veqter [3,4]. The contour method was also used on the nozzle mock-ups and was performed by Hill Engineering [5].

Both methods were used to find stresses in several locations in the mock-ups, but the measurements discussed here will be restricted to those measurements made along the through-thickness centerline of the DM weld areas of the mock-ups with no repair welds.

The two measurement techniques are different in practice as to their methods, but similar in that they cut away material, measure displacements due to assumed elastic residual stress relief, and then calculate the pre-cut stresses that would have been expected to produce those displacements. The techniques are described in more detail in their measurement reports [3,4,5] and in the three referenced papers [8,10,11]. A simple note distinguishing the use of DHD and iDHD is worth mentioning here. DHD is known to produce sometimes erroneous results in stress fields with high residual stresses approaching the range of the cut material's yield strength. This problem is caused by plastic deformation of the material when the measurement hole is drilled. The stress calculations are based on elastic material properties, and plastic behavior will cause errors in the calculation. In recent years a modification of the DHD method which uses an incremental approach to the cut/displacement combined measurement step has been used which has been demonstrated to produce more reliable results in high stress regions. The contour method also assumes elastic material behavior and is susceptible to stress calculation errors when stresses approach the material yield strength. The DHD measurements presented here apply the iDHD method as judged appropriate by those making the measurements to get the most reliable results in regions with high anticipated residual stresses.

While the DHD method uses a small drilled hole (1.5 mm) for measurements, leaving the part relatively intact, the Contour Method uses the wire electrical discharge machining (EDM) technique to create slices through the part revealing a plane to be measured. While this method provides a larger surface to measure, it can effectively measure stress in only one direction perpendicular to the cut plane, and leaves the part measured in pieces. For this reason, two mock-ups were measured.

Nozzle #2 was used in the pre stainless steel pipe weld state, and Nozzle #3 was used only in the post stainless steel pipe weld state. Obviously, variations in the welding of the two different DM welds were introduced by this necessity and must be considered. The DHD/iDHD measurements were taken before the nozzles were sectioned for the contour method.

The DHD/iDHD measurements to be shown here were taken from drilled holes in the centerline of the DM weld producing both axial and hoop stress measurements for each hole drilled. The contour method produces an entire plane to measure with each cut. The nozzles were cut axially into arcs as one would cut a pie producing two surfaces on which to measure hoop stresses through the DM weld thickness. Once these measurements were complete, the removed arc was then cut again on the transverse plane revealing an axial stress surface to measure. This surface passed through the center of the DM weld. The contour measurement report thus provided two hoop stress measurements for each nozzle, and a plane of axial stresses which was used to produce four separate through-thickness axial measurements at different clocked positions on the plane. The multiple hoop and axial stress contour

measurements were each averaged to simplify the presentation here.

PREDICTIONS AND MEASUREMENTS COMPARED

Figures 5 and 6 show the axial and hoop stress comparisons between the FEA predictions and the measurements produced by the two different methods. As with the previous prediction-only data, the average of all the data (predictions and measurements) is plotted as a thick blue line. The ± 3-standard deviation curves which encompass the data are plotted as thick red dashed lines. The FEA predictions were all performed on the same models representing both the Nozzle #2 and Nozzle #3 configuration, and as mentioned previously, the through-thickness stresses in the DM weld were found to be almost identical for the cases before and after application of the stainless steel pipe weld. Only the Nozzle #3 configuration FEA predictions are shown here because there is little or no difference from the Nozzle #2 results. The FEA predictions are plotted as thin lines as in the previous figures. Both Nozzle #2 and #3 measurement results were included in the comparisons to allow an examination of the measured differences found in the cases before and after the stainless steel pipe weld was completed that were found to be negligible in all of the FEA predictions.

The contour method measurements are indicated by thick orange and green lines while the DHD/iDHD measurements are indicated by orange and green dots. The green colored measurements are for the Nozzle #2 (pre SS-Weld) configuration and the orange colored measurements are for the Nozzle #3 (post SS-Weld) configuration.

The contour method Nozzle #2 and Nozzle #3 measurements look similar as though no significant change occurred due to the SS pipe weld application as the FEA models predicted. One must bear in mind that the measurements were made on two different nozzles while the FEA predictions were done on essentially one nozzle at two different steps in the manufacturing process. Variations in the measurements can be attributed to the difference in the actual nozzles measured rather than differences due to the application of the SS-Weld.

Overall the FEA predictions, contour method measurements and Nozzle #3 DHD/iDHD measurements show very similar trends. The DHD/iDHD measurements show a large difference in measured stress magnitude between the Nozzle #2 and #3 results that is not present in either the FEA predictions or the contour method measurements. Given the overall consistency of the other results, this suggests a potential artifact in the Nozzle #2 DHD/iDHD measurement results.

As an unbiased method to make a comparison of the predictions to the measurements, the average distance from the nozzle #3 measurements was calculated for each prediction and for the remaining measurements over the entire wall thickness. The overall average distances show that the axial stress predictions best match the contour method measurements [contour = 69 MPa (10 ksi) vs. iDHD = 131 MPa (19 ksi)] while the hoop stress predictions best match the iDHD measurements [contour = 154 MPa (22 ksi) vs. iDHD = 94 MPa (14 ksi)]. Further subdividing that comparison method, the predictions made using the kinematic hardening laws matched the measurements better in all cases except for the axial stress comparison with iDHD measurements where there was little difference in the overall match between the predictions with the two hardening laws.

As with the FEA predictions, the measurements show that the average inner diameter axial stress is near neutral and dipping into the compressive region until it becomes tensile at or before 50% through the thickness. It becomes neutral again at the outer diameter after rising to a peak at about 75% of the way through the thickness. The hoop stress graph shows the average of the stresses to be strongly compressive at the inner diameter and neutral to tensile at the outer diameter with the curves crossing into tension somewhat before 50% through the thickness from the inner diameter. The pre SS-Weld DHD/iDHD curve seems to not follow the trends of the other data.

The four FEA prediction curves from the models using isotropic hardening can be clearly distinguished from those using kinematic hardening. The effect is most noticeable in the axial stress graph (Figure 5.) where the isotropic models produce high axial compression stresses at 20% through the thickness, and high axial tension stresses at 80% through the thickness. The increase in tension stress toward the outer diameter seems to match what is indicated by the DHD/iDHD measurements for Nozzle #3. It is in this area of residual stress at or above the material's yield strength where the iDHD technique was applied in order to minimize potential plasticity induced measurement artifacts. FEA predictions with kinematic hardening fall almost exactly on both contour measurement curves along the entire data range. It should be noted that both DHD/iDHD and contour techniques are potentially susceptible to plasticity measurement artifacts at or near yield, making further comment on the accuracy of the measured residual stress profiles difficult.

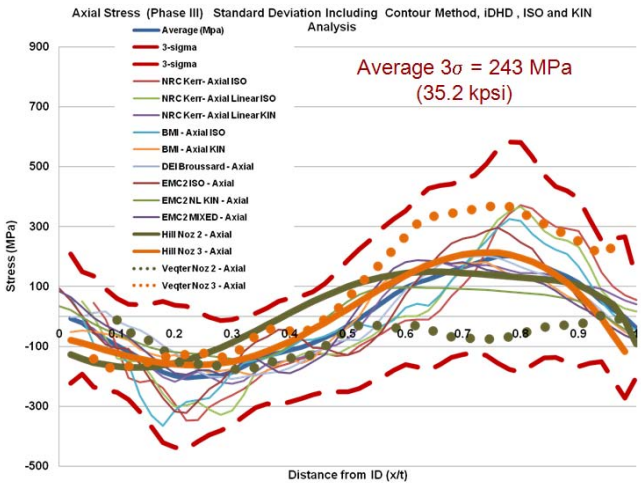

Figure 5. Axial Stress FEA Predictions and Measurements Compared

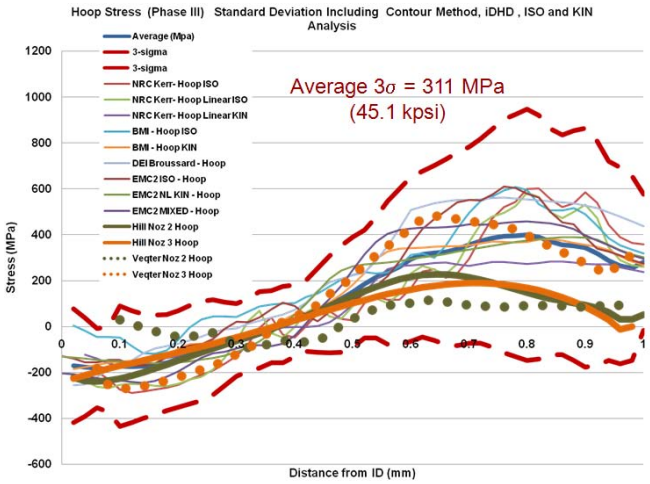

Figure 6. Hoop Stress FEA Predictions and Measurements Compared

The average ±3-standard deviation range for the axial stresses through the thickness is increased 25% from the prediction-only value of ±188 MPa (27.3 ksi) to ±235 MPa (34.1 ksi). Most of this increase can be attributed to the discrepancy between the Nozzle #2 and Nozzle #3 DHD/iDHD measurements toward the outer diameter. The average ± 3-standard deviation range for the hoop stresses through the thickness increased 28% from the prediction-only value ±243 MPa (35.2 ksi) to ±311 MPa (45.1 ksi).

All data is tabulated in Tables 1 and 2 at the end of this paper.

CONCLUSIONS

This analysis and measurement mock-up program has helped to improve the understanding of weld residual stresses in nuclear piping. The analyses and measurements have been used in part to validate stress based PWSCC mitigation techniques such as the Mechanical Stress Improvement Process [6], Full Structural and Optimized Weld Overlay [7]. and Inlays [12]. Results have allowed US NRC to provide input to MRP-169 on OWOL [13].

Also, the various predictions and measurements have shown which key aspects of various weld residual stress finite element predictive procedures have the greatest effect on results. Material hardening law behavior clearly has the most effect followed closely by the treatment of the annealing process in the welded material and material in the heat affected zone. The cross section weld macrograph appears to provide sufficient constraint to tune thermal models, as reasonable agreement with experimental results is achieved.

The analyses and measurements have also shown effects that are not solely of interest to finite element modelers, but are appropriate for manufacturing processes as well. The order of weld bead deposition, or weld sequencing can have a large effect on the stresses in the finished product. This work also shows the importance of the stainless steel weld to pipe system geometry, typically thought to have the beneficial effect of reducing the inner diameter stresses on the DM weld. A reduction in inner diameter stresses was not achieved in the geometry studied in the current work, but that fact adds to the knowledge of the effect of geometry and safe-end length on this usually beneficial effect.

When taken as a whole, the spread of data provided from measurements and predictions can be used to quantify the experimental and numerical uncertainly in claimed weld residual stress values. This statistical information will be valuable in probabilistic predictions used in the future.

ACKNOWLEDGMENTS

The authors would like to thank the US Nuclear Regulatory Commission and the Electric Power Research Institute for their support in this work.

REFERENCES

[1] Addendum to the Memorandum of Understanding (MOU) between NRC's Office of Nuclear Regulatory Research and Electric Power Research Institute, Inc. on Cooperative Nuclear Safety Research", NRC ADAMS Accession Number ML103490002, 2/15/2011

[2] Rudland, D., Kurth, R., Bishop, B., Mattie, P., Klasky, H., Harris, D., 2010 "Development of Compuatational Framework and Architecture for Extremely Low Probability of Rupture (XLPR) Code," ASME Pressure Vessels and Piping Conference, PVP2010-25963, Seattle, Washington.

[3] Bowman, D.,A., Deep-Hole "Drilling Residual Stress Measurements for the Joint EPRI & NRC Weld Residual Stress Research Program Phase 3 S&R Nozzle C," Veqter Report Number R09-011b, July, 2010.

[4] Bowman, D.,A., Deep-Hole "Drilling Residual Stress Measurements for the Joint EPRI & NRC Weld Residual Stress Research Program Phase 3 S&R Nozzle D," Veqter Report Number R09-011b/4, August, 2010.

[5] "Residual Stress Measurements on Nozzle #2 and Nozzle #3," Hill Engineering LLC Report Number HE102210, October, 2010.

[6] Fredette, L., Scott, P., M., Brust, F.W., 2008, "An Analytical Evaluation of the Efficacy of the Mechanical Stress Improvement Process in Pressurized Water Reactor Primary Cooling Piping," ASME Pressure Vessels and Piping Conference, PVP2008-61484, Chicago, Illinois.

[7] Fredette, L., Scott, P., M., Brust, F.W., Csontos, A., 2009, "An Analytical Evaluation of the Full Structural Weld Overlay as a Stress Improving Mitigation Strategy to Prevent Primary Water Stress Corrosion Cracking in Pressurized Water Reactor Piping," ASME Pressure Vessels and Piping Conference, PVP2009-77327, Prague, Czech Republic.

[8] Ogawa, K., Chidwick, L., A., Kingston, E., J., Muroya, I., Iwamoto, Y., Smith, D., J., 2009, "Measurement of Residual Stresses in the Dissimilar Metal Weld Joint of a Safe-End Nozzle Component," ASME Pressure Vessels and Piping Conference, PVP2009-77830, Prague, Czech Republic.

[9] Rudland, D., Zhang, T., Wilkowski, G., Csontos, A., 2008 "Welding Residual Stress Solutions for Dissimilar Metal Surge Line Nozzles Welds," ASME Pressure Vessels and Piping Conference, PVP2008-61285, Chicago, Illinois.

[10] Mahmoudi, A-H., Smith, D., J., Truman, C., E., Pavier, M., J., 2009, "Application of the Modified Deep Hole Drilling Technique (iDHD) for Measuring Near Yield Non-Axisymmetric Residual Stresses," ASME Pressure Vessels and Piping Conference, PVP2009-77940, Prague, Czech Republic.

[11] Dennis, R., J., Leffatt, N., A., Kutarski, E., A., 2009, "Investigation of the Performance of the Contour Residual Stress Measurement Method when Applied to Welded Pipe Structures," ASME Pressure Vessels and Piping Conference, PVP2009-77470, Prague, Czech Republic.

[12] Rudland, D., Csontos, A., Brust, F., Zhang, T., 2009, "Welding Residual Stress and Flaw Evaluation for Dissimilar Metal Welds with Alloy 52 Inlays," ASME Pressure Vessels and Piping Conference, PVP2009-77167, Prague, Czech Republic.

[13] King, C., Frederick, G., 2005, "Non-Proprietary Version, Materials Reliability Program: Technical Basis for Preemptive Weld Overlays for Alloy 82/182 Butt Welds in PWRs (MRP-169)," EPRI Report Number 1012843, Electric Power Research Institute, Palo Alto, CA.

[14] ABAQUS, V6.7-1, 2007, Dassault Systèmes, Providence, RI.

[15] ANSYS Inc., 2009, Canonsburg, PA.

Table 1. Axial Stress, Through-Thickness Prediction and Measurement Data

	FEA Axial Stress Predictions (MPa)									Axial Stress Measurements (MPa)			
x/t	NRC Kerr-Axial ISO	NRC Kerr-Axial Linear ISO	NRC Kerr-Axial Linear KIN	BMI - Axial ISO	BMI - Axial KIN	DEI Broussard - Axial	EMC2 ISO – Axial	EMC2 NL KIN - Axial	EMC2 MIXED - Axial	Hill Noz 2 - Axial	Hill Noz 3 - Axial	Veqter Noz 2 - Axial	Veqter Noz 3 - Axial
0.00							93	35	83				
0.02				63	-52	-3	54	21	64	-128	-78		
0.04		50	-20	-3	-48	-1	3	-2	31	-141	-89		
0.06	45	0	-41	-91	-51	12	-52	-25	-3	-153	-100		-142
0.08	-9	-73	-82	-103	-59	16	-93	-44	-30	-161	-112		-169
0.10	-102	-139	-127	-114	-66	-16	-107	-60	-49	-167	-123	-13	-173
0.12	-205	-150	-140	-157	-78	-33	-108	-74	-70	-170	-133	-52	-167
0.14	-219	-150	-145	-264	-110	-45	-159	-90	-102	-170	-142	-67	-160
0.16	-214	-199	-172	-330	-126	-68	-217	-104	-134	-168	-149	-85	-149
0.18	-240	-259	-202	-365	-134	-97	-273	-114	-164	-163	-156	-110	-137
0.20	-291	-301	-217	-314	-129	-120	-317	-119	-190	-155	-160	-147	-130
0.22	-348	-297	-201	-285	-149	-150	-322	-122	-194	-146	-162	-158	-127
0.24	-346	-284	-185	-279	-175	-181	-283	-126	-180	-133	-163	-158	-123
0.26	-302	-311	-201	-273	-186	-201	-241	-131	-179	-119	-160	-154	-122
0.28	-280	-328	-219	-234	-182	-201	-218	-137	-194	-104	-156	-170	-136
0.30	-263	-313	-225	-186	-176	-209	-175	-142	-183	-86	-150	-177	-129
0.32	-242	-262	-214	-155	-190	-202	-117	-144	-149	-68	-141	-177	-102
0.34	-214	-184	-184	-147	-197	-195	-86	-143	-139	-48	-130	-169	-65
0.36	-179	-158	-159	-138	-181	-189	-67	-136	-164	-28	-117	-156	-42
0.38	-167	-154	-152	-126	-159	-184	-44	-121	-186	-8	-101	-145	-42
0.40	-156	-145	-147	-103	-142	-171	-46	-99	-189	12	-83	-139	-49
0.42	-142	-127	-136	-80	-155	-152	-74	-72	-174	32	-64	-139	-57
0.44	-128	-114	-121	-78	-141	-125	-104	-41	-150	51	-43	-125	-37
0.46	-124	-127	-106	-66	-98	-101	-106	-8	-126	68	-21	-99	-9
0.48	-132	-127	-95	-48	-63	-83	-121	22	-78	84	2	-69	21
0.50	-129	-106	-74	-31	-36	-77	-129	51	-20	100	25	-46	59
0.52	-98	-86	-38	-25	1	-79	-116	73	33	112	49	-30	108
0.54	-77	-68	12	-34	62	-48	-87	87	79	123	72	-25	141
0.56	-56	-41	65	-32	109	-2	-49	93	123	132	95	-34	183
0.58	-32	-6	104	-12	139	43	11	96	160	139	116	-38	225
0.60	-14	1	129	29	149	89	74	97	181	144	137	-34	267
0.62	-11	1	154	42	163	119	120	97	188	147	155	-30	309
0.64	-11	20	174	36	184	148	168	96	186	149	172	-40	331
0.66	21	65	181	71	184	173	209	95	181	149	186	-60	338
0.68	68	121	171	119	177	192	243	93	177	148	198	-68	345
0.70	104	156	163	167	176	197	259	92	181	145	207	-72	351
0.72	149	207	171	213	178	201	268	90	170	143	212	-73	358
0.74	218	271	172	252	181	202	284	88	156	140	214	-75	365
0.76	300	322	165	295	161	195	296	85	149	136	213	-74	372
0.78	343	351	154	325	140	182	276	82	143	133	206	-68	367
0.80	372	367	144	319	129	166	246	79	132	130	196	-59	348
0.82	360	333	145	275	132	151	226	76	120	127	183	-45	329
0.84	326	286	144	244	119	138	174	72	107	124	163	-35	310
0.86	299	261	133	223	93	121	130	67	85	120	140	-29	290
0.88	293	252	118	209	68	103	110	61	59	114	113	-30	271
0.90	285	233	104	167	50	79	60	52	35	105	78	-27	252
0.92	224	167	100	110	33	54	12	36	15	86	38	-17	227
0.94	148	87	93	49	13	20	-13	9	-11	63	-6	4	206
0.96	100	48	73	7	-21	-15	-40	-19	-39	41	-61	-4	232
0.98	71	27	54	-24	-51	-46	-64	-42	-64	-13	-117	-12	243
1.00	55	17	40	-45	-70	-77	-78	-55	-79	-92			

Table 2. Hoop Stress, Through-Thickness Prediction and Measurement Data

	FEA Hoop Stress Predictions (MPa)									Hoop Stress Measurements (MPa)			
x/t	NRC Kerr-Hoop ISO	NRC Kerr-Hoop Linear ISO	NRC Kerr-Hoop Linear KIN	BMI - Hoop ISO	BMI - Hoop KIN	DEI Broussard - Hoop	EMC2 ISO – Hoop	EMC2 NL KIN - Hoop	EMC2 MIXED - Hoop	Hill Noz 2 - Hoop	Hill Noz 3 - Hoop	Veqter Noz 2 - Hoop	Veqter Noz 3 - Hoop
0.00							-129	-130	-202				
0.02				4	-185	-256	-139	-134	-207	-223	-227		
0.04		-237	-123	-18	-176	-252	-156	-140	-215	-236	-211		
0.06	-196	-261	-138	-45	-165	-219	-156	-145	-225	-238	-197		-183
0.08	-228	-268	-160	-46	-158	-186	-145	-149	-232	-234	-184		-255
0.10	-275	-253	-172	-47	-151	-174	-145	-152	-236	-226	-171	29	-272
0.12	-289	-250	-161	-84	-149	-147	-168	-156	-241	-213	-159	13	-267
0.14	-283	-251	-146	-116	-153	-115	-171	-159	-246	-199	-147	-5	-261
0.16	-274	-258	-141	-117	-144	-95	-161	-161	-237	-183	-136	-20	-248
0.18	-266	-259	-137	-104	-128	-85	-136	-160	-217	-165	-124	-33	-234
0.20	-254	-250	-128	-59	-95	-74	-102	-157	-195	-148	-112	-45	-219
0.22	-230	-231	-105	-5	-76	-61	-83	-151	-167	-130	-99	-44	-203
0.24	-210	-218	-82	31	-73	-43	-76	-144	-135	-113	-87	-36	-186
0.26	-191	-187	-77	45	-72	-25	-54	-136	-116	-95	-74	-28	-171
0.28	-163	-137	-74	44	-55	-13	-9	-126	-109	-79	-60	-53	-149
0.30	-129	-61	-69	43	-35	-8	21	-110	-96	-62	-46	-76	-121
0.32	-76	24	-58	66	-33	12	20	-91	-83	-45	-32	-91	-97
0.34	-7	70	-40	88	-27	26	39	-64	-82	-28	-18	-86	-58
0.36	40	-29	-15	97	-3	39	75	-29	-86	-11	-3	-72	-14
0.38	-35	-48	-4	101	27	52	104	10	-74	8	12	-62	21
0.40	-46	-1	-1	103	54	74	91	53	-39	27	28	-59	45
0.42	2	62	-1	128	60	105	48	101	14	47	43	-68	61
0.44	56	90	3	143	74	157	22	153	71	68	58	-59	96
0.46	67	44	19	175	108	194	65	208	121	90	73	-35	142
0.48	34	33	52	205	140	208	90	243	177	112	88	6	177
0.50	28	88	95	225	182	222	113	262	246	134	102	34	217
0.52	103	127	149	238	233	236	142	270	315	154	116	57	270
0.54	132	124	205	232	294	285	177	275	370	174	129	80	310
0.56	117	101	249	236	326	350	220	280	405	191	141	91	350
0.58	118	142	264	264	341	428	284	286	421	206	152	98	390
0.60	167	232	267	313	341	508	361	293	427	216	162	103	430
0.62	241	264	272	318	344	523	426	301	431	224	170	114	470
0.64	250	247	278	300	348	538	469	309	432	228	178	115	483
0.66	213	230	279	352	349	546	505	317	434	227	183	108	476
0.68	231	273	271	427	349	552	542	326	437	224	187	99	468
0.70	297	370	265	496	354	552	552	336	445	215	189	94	460
0.72	388	445	274	549	362	554	549	345	444	205	190	90	453
0.74	472	478	281	566	370	561	576	353	445	192	188	87	445
0.76	520	495	282	592	368	562	610	361	452	177	184	87	438
0.78	543	524	278	609	366	559	604	368	457	162	178	88	423
0.80	600	582	273	595	368	554	579	375	458	147	169	92	398
0.82	602	564	276	534	379	549	563	381	455	134	158	93	373
0.84	557	499	282	506	380	546	500	386	449	122	144	92	349
0.86	520	474	283	506	375	542	454	389	440	112	128	89	324
0.88	538	499	278	517	365	536	446	390	424	103	109	86	300
0.90	585	532	272	489	356	527	391	387	399	94	86	85	275
0.92	540	473	272	440	347	516	340	378	375	81	59	88	249
0.94	443	347	271	384	333	497	328	357	355	62	29	98	229
0.96	390	291	260	355	307	478	310	334	332	31	-11	93	279
0.98	366	266	248	335	284	458	290	314	310	32	0	89	313
1.00	357	260	238	319	269	438	276	302	295	52			